Slope angle versus slope height – the basis of an empirical tool for slope design within fractured rock masses using IUCM

T.D. Styles
Mining One Consultants / Cavroc, Ashbourne, United Kingdom
tstyles@miningone.com.au

A. Vakili
Mining One Consultants / Cavroc, Melbourne, Australia

Abstract

The presentation of slope angle versus slope height charts remains one of the most useful ways to present slope design data. This research is the culmination of many simulations with varying overall slope angles. The culmination of these is a slope angle versus slope height chart with curves that define the factor of safety for specific rock mass conditions (referred to as 'Slope Stability Curves').

Slope Stability Curves are presented that are intended to be an initial guide to slope design within the chosen rock mass conditions based on the Geological Strength Index (GSI) coupled with the Hoek-Brown criterion. The variance of results and the implication to the preliminary slope design, is studied with respect to different rock mass strength criteria. In particular, the results advocate the use of the recently developed 'Improved Unified Constitutive Model' (IUCM). This takes the best parts of Mohr-Coulomb and Hoek-Brown, with integrated confinement-controlled softening/hardening of cohesion and friction, confinement-controlled changes in the dilation angle, and porosity-controlled modulus softening.

Keywords

Slope Stability, Slope angle versus slope height charts, Hoek-Brown, Numerical Modelling

ISRM

NBG

1 Introduction

The stability of slopes in fractured rock masses is a challenging area of study, motivated by the increasing demand to provide safe and realistic forecasts of stability, particularly in engineered slopes. For open pit mines, the dominant failure modes are summarised in Fig. 1. This paper is concerned with overall or inter-ramp failure, where instability is a complex interaction between the intact rock strength, fracture network (incipient joints sets and bedding), i.e. more 'mass'/continuum-controlled behaviour. The concepts in this paper are not intended for slopes where either large-scale structural features such as faults or weak lithologies provide a preferential pathway for failure.

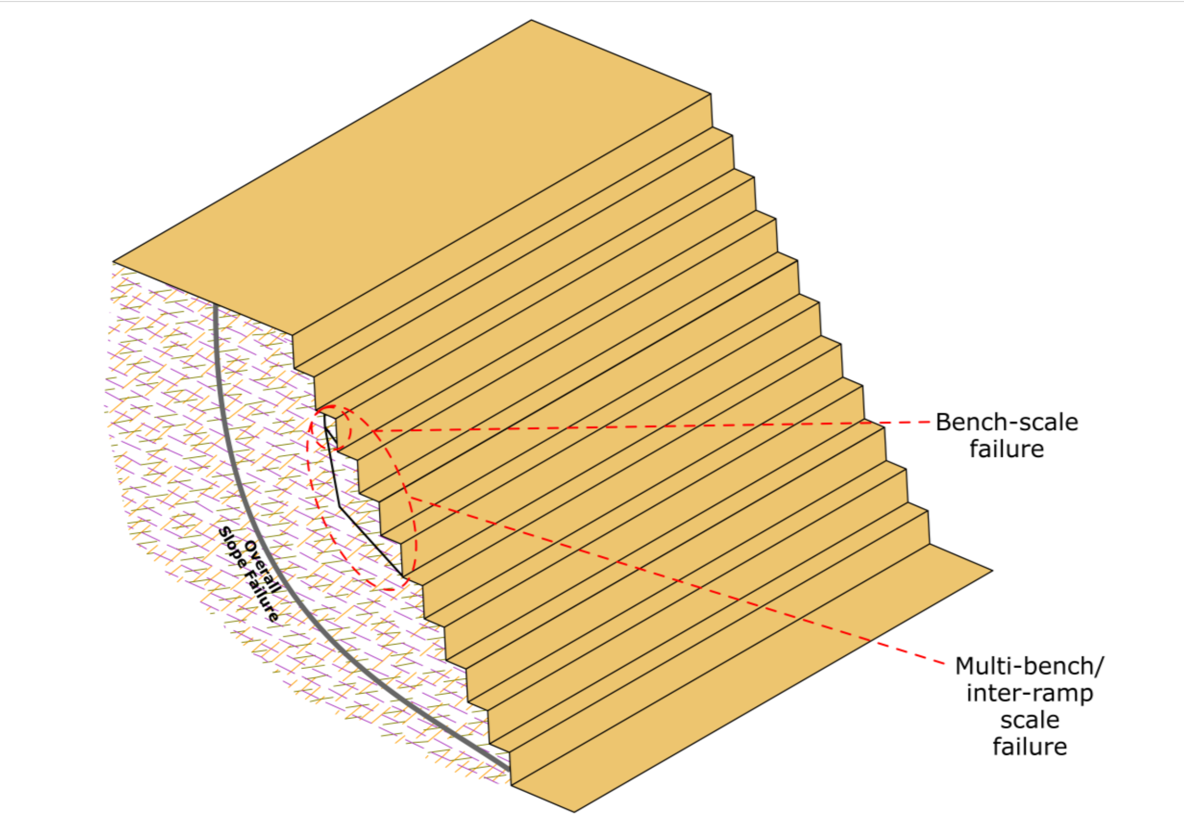

Fig. 1 Failure modes in a fractured rock mass, considering discontinuity-controlled bench/inter-bench scale failure mechanisms and mass-controlled overall slope failure (image developed alongside Land and Minerals Consulting Limited)

The following sections discuss the slope angle versus slope height charts that are currently available. Subsequently 'Slope Stability Curves' are introduced, which are plotted on a chart with slope angle versus slope height, for a specific rock mass condition. The method of numerical analysis that has been used to develop the curves is also briefly outlined, prior to an introduction to the conceptual cases that have been analysed, and the subsequent results.

1.1 Slope angle versus slope height

An empirical graph that presents the relationship between slope height and slope angle is one of the most useful ways to present slope design data (Fig. 2); however, one should not use such charts as a basis of design (Hoek and Bray, 1981). Instead, a chart which forecasts the stability for a specific slope height and angle should be considered as a useful and quick to use tool that can be used to either provide an initial guide for slope design or as a reference to study the influence of inputs on analysis results.

The most well-known slope height versus slope angle charts are presented in Hoek and Bray (1981) and Sjöberg (1999). Note that Sjoberg classified the ISRM qualitative rock strength for each case study. As shown in Fig. 3a, Hoek and Bray (1981) developed their chart on stable and unstable slopes that had been observed in Spain. The more well-known coloured chart for this data is presented in Read and Stacey (2009), Fig. 3b. To illustrate the potential variability in this approach, a particular slope from Kanmantoo Copper Mine can be plotted to have a Factor of Safety (FS) <1 on the Hoek and Bray (1981) chart; in contrast, Lucas at al. (2020) suggests a FS of 1.4 for the particular slope at Kanmantoo Copper Mine, as verified by monitoring.

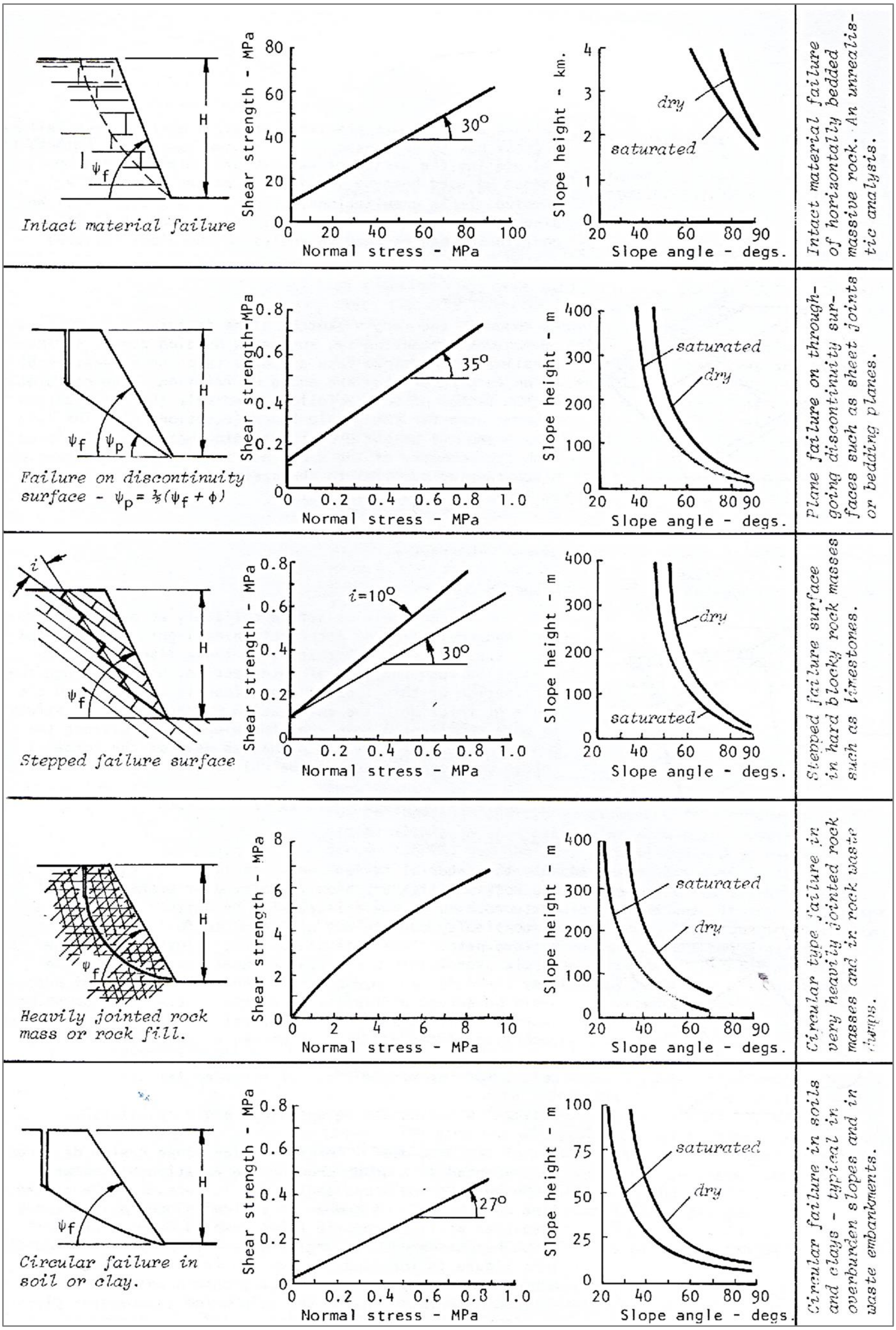

Fig. 2 Slope angle versus slope height charts for different materials (after Hoek and Bray, 1981)

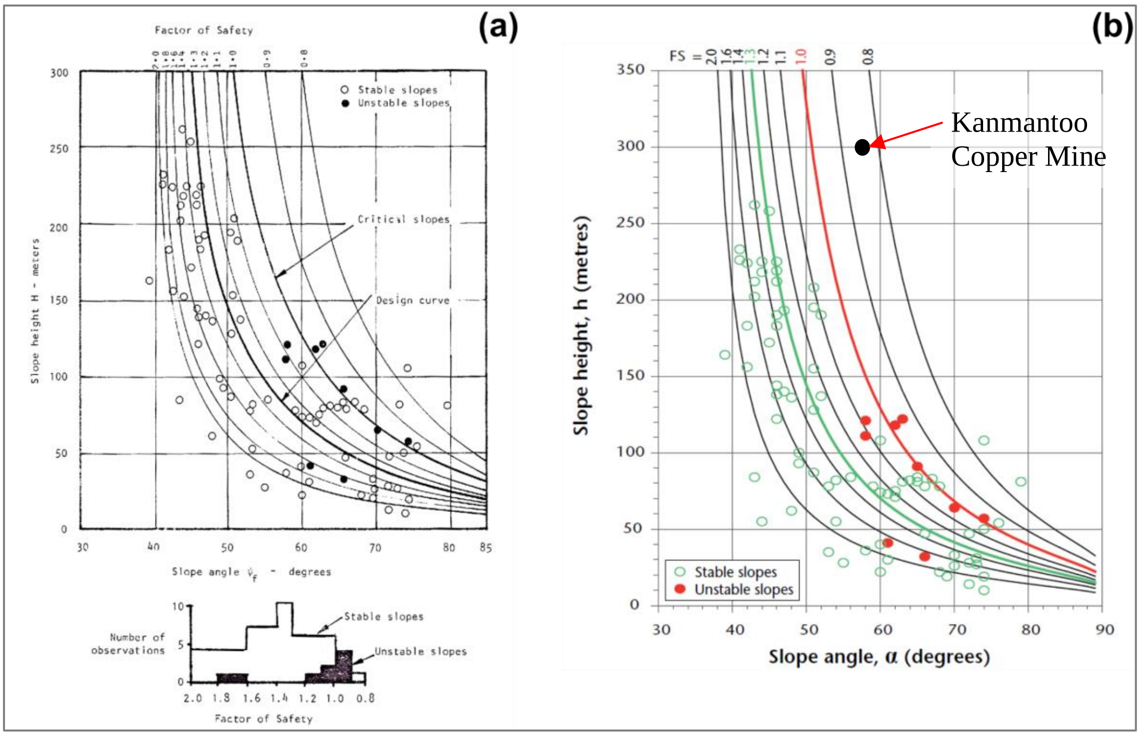

Fig. 3 (a) Slope angle versus slope height chart with for FOS best fit lines, for porphyry slopes in the Rio Tinto area, Spain (after Hoek and Bray, 1981); (b) the reproduced coloured version of the chart presented in Read and Stacey (2009) with an additional data point from a recent analysis

In general slope angle versus slope height charts presented are intended to be generic in that they are developed from failures in a mixture of conditions, with no specific guidance on variability with differing rock mass strength. Haines and Terbrugge (1991) present slope angle versus slope height in the form of a design chart, which allows the classification of slope geometry based on MRMR and specifies when additional analysis is required. This provides an initial guide and addresses the variability with differing rock mass strength. However, slope height is limited to 300 m and its application has become restricted, considering that the Geological Strength Index (GSI) is now the most favoured method of rock mass classification.

The most recent development of slope angle versus slope height charts is from Carter (2018), who presented a slope angle versus slope height chart with classification of the Hoek-Brown constant, m_b (Fig. 4). Conditions are inferred for slopes up to 1500 m in height, and Carter (2018) suggests an association with the U-shaped Jaeger curves, which typically define the anisotropic effect in rock.

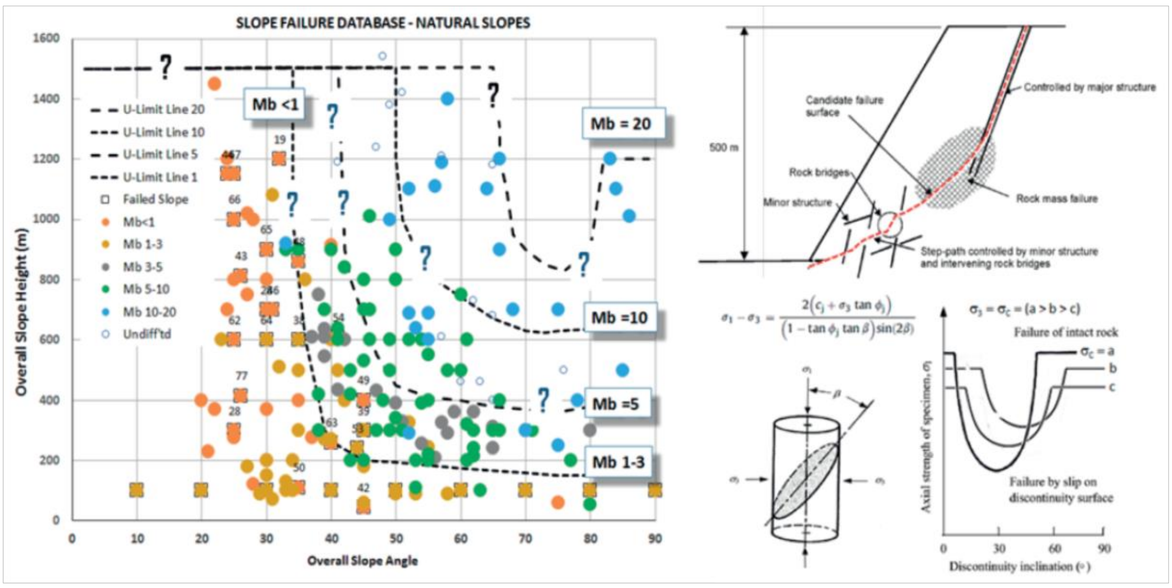

Fig. 4 Carter's (2018) indication of maximum slope heights for a given rock type and slope configuration (a) Slope angle versus slope height chart natural slopes, (b) Hoek et al. (2000) failure surface resulting from a composite failure mechanism (from); (c) modified Jaeger (1960) and Hoek & Brown (1980) material strength variability with orientation of anisotropy possibly related acting as control on stable slope configuration (after Carter 2018).

1.2 'Slope Stability Curves'

To provide an initial and simplified guide for assessing slope stability, numerous stability analyses have been completed in 2D, presenting the FS for different slope geometries in a plane strain state. The culmination of these is a slope angle versus slope height chart with FS curves for a specific rock mass conditions (referred to as 'Slope Stability Curves').

Importantly a slope stability curve chart is intended to represent the 'composite' failure mode, where a single geological unit controls the behaviour of the slope; i.e. there are no specific features such as faults or weak lithologies providing a preferential pathway for failure. The slope stability curve represents a generic rock mass condition, characterised using the Geological Strength Index (GSI) coupled with the Hoek-Brown criterion.

The curves have been developed using SlopeExamine (developed by Cavroc), in which there is an in-built constitutive model known as the 'Improved Unified Constitutive Model' (IUCM). This is a non-proprietary method that takes the best parts of the Mohr-Coulomb and Hoek-Brown failure criteria, as described in detail by Vakili (2016). It has been designed to capture the transition from brittle to ductile response, with confinement-dependent strain-softening and dilatational response. It also explicitly considers anisotropy.

1.3 SlopeExamine / SlopeX

SlopeExamine (also known as SlopeX), has been developed by Cavroc and is a plug-in to FLAC3D (the finite difference code developed by Itasca). The plug-in automates the meshing and generates a simulation-ready input file that can be solved within FLAC3D. SlopeX is controlled through a user interface which has been designed to minimise the difficulty and the time that is typically taken during the development of an advanced numerical model. The plug-in is introduced in detail in Vakili et al. (2020).

The user interface provides step-by-step guidance so that no specialist knowledge is required. This increases the usability of an advanced numerical model for beginner to intermediate users. To define the inbuilt constitutive model (IUCM), only five input values are required providing a streamlined approach:

- Density
- Intact Young's Modulus
- GSI
- Hoek-Brown constant m_i
- Uniaxial Compressive Strength (UCS)

Note that in addition to the above, there are three inputs that can be entered to control the residual behaviour (cohesion, friction and tension), and a value that controls the critical strain for strain-softening behaviour. Typically, these values do not need altering as in most cases the default values for residual strength are appropriate. The critical strain value is automatically calculated based on GSI value and the zone size. However, if calibration data exists, the critical strain value can be increased or decreased.

IUCM includes a further two values that control the magnitude of anisotropy, which is represented in the model using ubiquitous joints. This model was developed to be detailed and versatile; and it has been calibrated and verified against over 100 mining cases worldwide. A recent selection of validation cases is presented by Ford et al. (2020), with detail on one particular case by Lucas at al. (2020).

1.4 Blast Damage and Strain Softening

Slope stability analyses by a conventional Generalized Hoek-Brown approach, usually incorporates a disturbance factor ('D factor'). This downgrades the rock mass strength to account for relaxation that results from blasting, as well as the extraction itself (i.e. strain-softening effect). However, the magnitude and extent to which blast damage should extend into the rock mass is a contentious issue, with limited guidance available.

By its nature using the IUCM considers the relaxation (strain-softening) of a rock mass due to mining induced stress. As discussed by Vakili (2016), this component of the D factor assumption carries the largest weight (approximately 70%), in comparison to the much smaller influence of blasting itself. To avoid applying such a degradation to IUCM, which explicitly considers strain-softening, blast damage has not been included. It is suggested that the overall stability of the slope is not influenced by the blast induced damage which is typically applicable for bench-scale to inter-ramp stability.

Recent guidance by Silva and Gómex (2015) suggests a 'surface band' in which the value of D varies linearly, with a high value at the slope surface reducing to a low value further back in the slope where there is less damage. The thickness of the damaged zone increases with depth, with a maximum of ⅓ of the slope height (Silva and Gómex, 2015). Cancino et al. (2018) use this in conjunction with a strain-softening strength criterion known as 'CaveHoek'; sensitivity analyses are presented suggesting appropriate values for the following inputs that are necessary for CaveHoek.

- Critical strain multiplier, which is the plastic strain at which the rock mass strength reduces from peak to residual strength;
- Dilation angle, this controls the behaviour of the material once it is at its residual strength.

It is of note that when using the IUCM, the critical strain is automatically calculated using the GSI value and the zone size. Also, the dilation angle is determined using the relationship proposed by Alejano and Alonso (2005). Their relationship estimates the current peak dilation angle, as a function of the acting confining stress, internal friction angle and the UCS. The dependency of dilation on the acting confining stress produces high dilation angles at low confinement, and low dilation angles at high confinement. The dilation angle also softens within the IUCM, ultimately reducing to zero.

Cancino et al. (2018) compare their CaveHoek model to a more conventional modified Hoek-Brown model, both with the surface band of damage. Fig. 5 shows their suggested result, which indicates a lower factor of safety (FS) and subsequent failure surface within the disturbed surface band. To conform with the overall slope failure mechanism in which a deeper failure surface is considered, the surface band of damage has not been applied within this research. Instead, it is suggested that if the intended slope failure mechanism is relatively shallow and blast induced damage, then a numerical modelling should be used to resolve the FS.

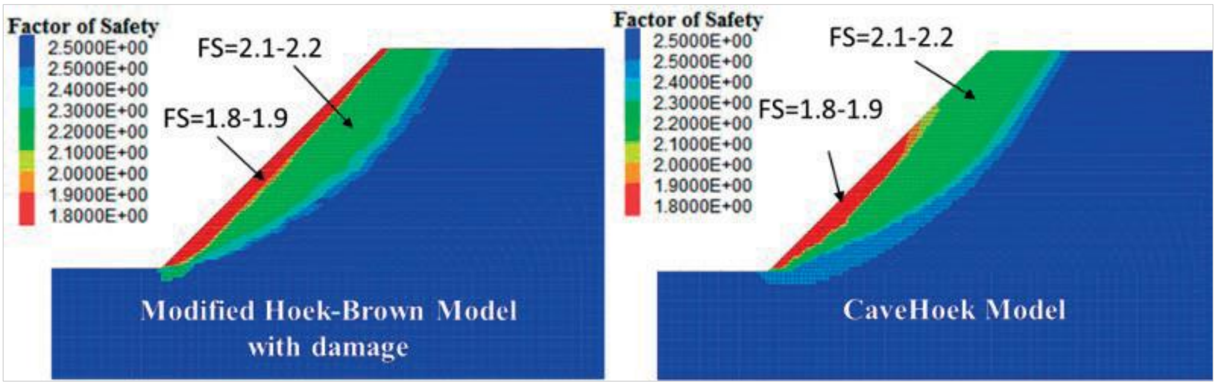

Fig. 5 Comparison of strain softening model with a conventional modified Hoek-Brown analysis for a 500 m high slope with an a slope angle of 45° analysed within a rock mass of 'moderate quality; both models include the a blast damaged zone (after Cancino et al., 2018)

Recently, McKenzie (2016) provided an objective view of the impact of blasting near open pit walls. As suggested, numerical modelling can 'probably' estimate the blast damage factor. However, the width of the blast damage zone should perhaps be associated with the critical peak particle velocity for the rock mass, which in turn is controlled by the configuration of the blast. This suggests that to capture the effect of blasting itself, it would be necessary to complete detailed and specific analyses for each unique set of conditions.

2 Parameters and Conditions

2.1 Model Geometry

As discussed in Section 1.2, for this research, the analyses were completed in two-dimensions. SlopeX was used to generate the model with an octree mesh rapidly. The size of each zone is automatically calculated in SlopeX, which places a smaller zone size in the area of interest to suffice the conditions specified in Read and Stacey (2009). Further from the slope, the size of the elements is coarser helping to reduce the computation time.

With a variability of zone sizes, the 2D slice is governed by the largest element along the boundaries of the model. Examples of the models are provided in Fig. 6; note that proximity of the boundaries follow or exceed the guidelines suggested in Read and Stacey (2009).

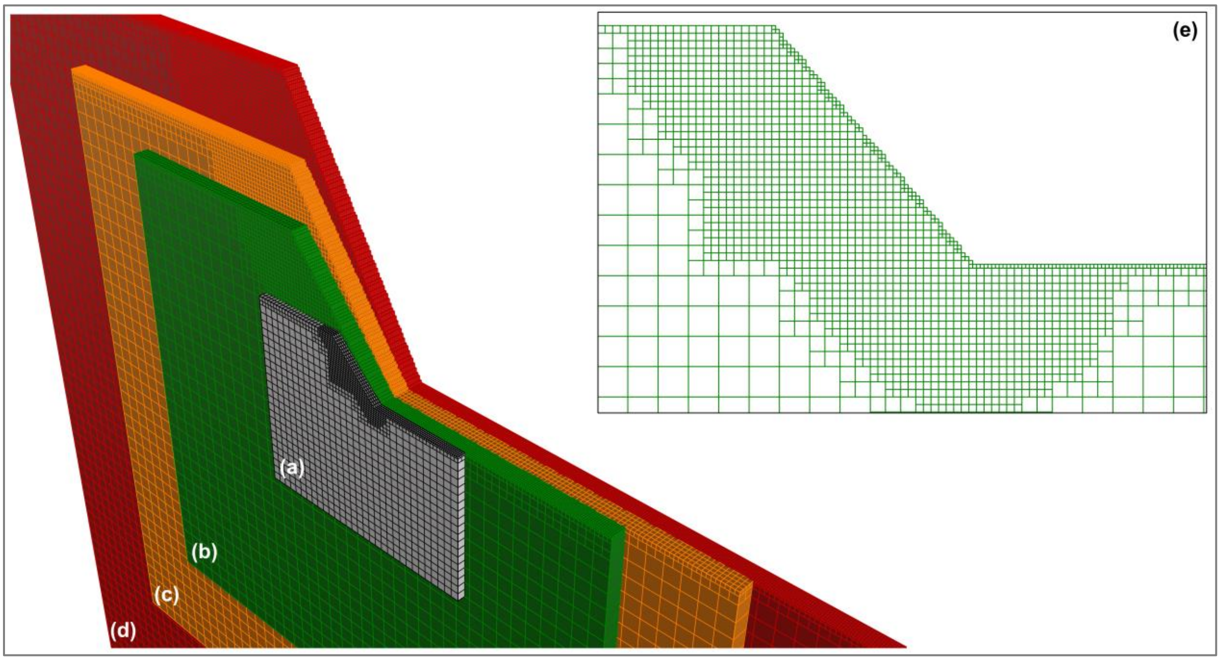

Fig. 6 Perspective views of (a) 200 m high slope with a slope angle of 45°; (b) 500 m high slope with a slope angle of 50°; (c) 700m high slope with a slope angle of 55°; (d) 1000m high slope with a slope angle of 60°; (e) side view of a 500 m high slope with a slope angle of 50°

SlopeX can incorporate a representation of the groundwater into the model, however as part of these initial analyses this functionality has not been applied. In this case it was considered that in order to analyse many scenarios, in the first instance fully drained conditions were preferred. As part of the project development, it is intended that charts will be developed to represent the groundwater in the same as in the circular failure charts presented by Hoek and Bray (1981).

2.2 Conceptual Rock Masses

Three rock masses have been chosen to represent a range of conditions (Table 1
Table 1). Rock Mass A and Rock Mass B were selected so that they can be plotted on the chart defining the Hoek-Brown Classification system (Fig. 7). Rock Mass C is based on the conditions within a large open pit and relatively steep slopes, where the stability is largely governed by a single lithology. The classification of the rock mass leaves it with surface conditions that can be considered to be between 'fair' and 'good' and therefore it plots between the two categories. The following summaries the three cases that are represented:

- Rock Mass A can be considered as a moderate rock mass with a 'very blocky' structure and 'fair' surface conditions (area coloured orange on Fig. 7), this could be a limestone with a moderate to relatively low Young's Modulus;
- Rock Mass B can be considered as a poor rock mass with a 'blocky/seamy' structure' and 'fair' surface conditions (area coloured red on Fig. 7), although the UCS is relatively low and perhaps not representative of the intact material; and,
- Rock Mass C can be considered as a relatively strong rock mass with a 'blocky' structure and surface conditions that are between 'fair' and 'good' (area coloured green on Fig. 7), this is based on a metamorphic rock (medium amorphous).

Table 1 Model inputs for chosen rock mass conditions

Parameter		Rock Mass A	Rock Mass B	Rock Mass C
Density	ρ (t/m^3)	2.7	2.7	2.7
Intact Young's Modulus	E_i (GPa)	30.0	28.2	78
Geological Strength Index	GSI	50	40	69
Hoek Brown Constant	m_i	16	10	25
Intact uniaxial compressive strength	UCS (MPa)	50	20	119

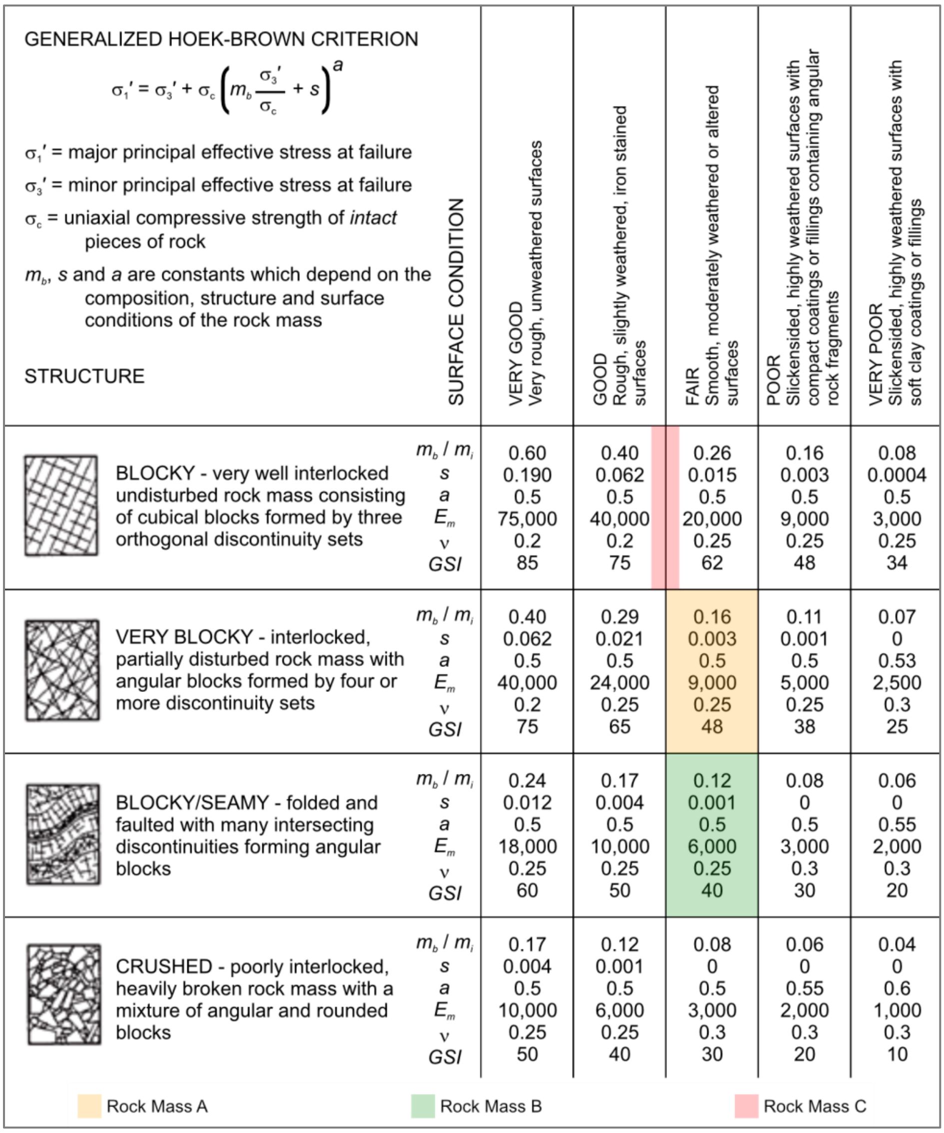

GENERALIZED HOEK-BROWN CRITERION

$$\sigma_1' = \sigma_3' + \sigma_c \left(m_b \frac{\sigma_3'}{\sigma_c} + s \right)^a$$

σ_1' = major principal effective stress at failure

σ_3' = minor principal effective stress at failure

σ_c = uniaxial compressive strength of *intact* pieces of rock

m_b, s and a are constants which depend on the composition, structure and surface conditions of the rock mass

STRUCTURE	SURFACE CONDITION	VERY GOOD Very rough, unweathered surfaces	GOOD Rough, slightly weathered, iron stained surfaces	FAIR Smooth, moderately weathered or altered surfaces	POOR Slickensided, highly weathered surfaces with compact coatings or fillings containing angular rock fragments	VERY POOR Slickensided, highly weathered surfaces with soft clay coatings or fillings
BLOCKY - very well interlocked undisturbed rock mass consisting of cubical blocks formed by three orthogonal discontinuity sets	m_b / m_i	0.60	0.40	0.26	0.16	0.08
	s	0.190	0.062	0.015	0.003	0.0004
	a	0.5	0.5	0.5	0.5	0.5
	E_m	75,000	40,000	20,000	9,000	3,000
	ν	0.2	0.2	0.25	0.25	0.25
	GSI	85	75	62	48	34
VERY BLOCKY - interlocked, partially disturbed rock mass with angular blocks formed by four or more discontinuity sets	m_b / m_i	0.40	0.29	0.16	0.11	0.07
	s	0.062	0.021	0.003	0.001	0
	a	0.5	0.5	0.5	0.5	0.53
	E_m	40,000	24,000	9,000	5,000	2,500
	ν	0.2	0.25	0.25	0.25	0.3
	GSI	75	65	48	38	25
BLOCKY/SEAMY - folded and faulted with many intersecting discontinuities forming angular blocks	m_b / m_i	0.24	0.17	0.12	0.08	0.06
	s	0.012	0.004	0.001	0	0
	a	0.5	0.5	0.5	0.5	0.55
	E_m	18,000	10,000	6,000	3,000	2,000
	ν	0.25	0.25	0.25	0.3	0.3
	GSI	60	50	40	30	20
CRUSHED - poorly interlocked, heavily broken rock mass with a mixture of angular and rounded blocks	m_b / m_i	0.17	0.12	0.08	0.06	0.04
	s	0.004	0.001	0	0	0
	a	0.5	0.5	0.5	0.55	0.6
	E_m	10,000	6,000	3,000	2,000	1,000
	ν	0.25	0.25	0.3	0.3	0.3
	GSI	50	40	30	20	10

Rock Mass A — Rock Mass B — Rock Mass C

Fig. 7 Chart from Hoek et al. (1996) which has estimates of Hoek-Brown constants; the conditions for the conceptual rock masses are overlaid (Rock Mass C is between 'fair' and 'good' with higher Young's Modulus)

2.3 Failure Criteria

Primarily the Slope Stability Curves are based on FS, with the division of three categories that represent the category and consequence of failure (Table 2). Lorig and Varona (2000) suggest displacement and velocity data in a numerical model should be used to indicate stability, in much the same way as prism data from monitoring in open pits. Increasing displacements and velocities indicate an unstable situation; steady displacements and decreasing velocities indicate a stable situation. Lorig and Varona (2000) found that velocities below 1×10^{-6} m/s indicate stability in FLAC3D, whereas velocities above 1×10^{-5} m/s indicate instability. Mining One's experience of back analysis in several other sites has shown that:

- A velocity greater than 1×10^{-5} m/s (after model is fully converged), represents a progressive or transitional system (regressive and then progressive);
- A velocity of less than 1×10^{-7} m/s (after model is fully converged), represents a regressive stable system; and,
- A velocity between 1×10^{-7} m/s to 1×10^{-5} m/s represent a regressive but slow-moving system.

It is important to note that velocity is per modelling timestep and is not correlated with real time, but by calibrating to actual slope movement it can be indicatively related to actual slope velocity (for slow-moving slopes). The authors suggest that this velocity criterion is only suitable to predict deep seated failure at overall or inter-ramp scale, and it is not suitable for prediction of bench-scale failure.

Table 2 Acceptance criteria after modified after Pine (1992)

Category & Consequence of Failure	Examples	Mean Factor of Safety
Not Serious	Temporary slopes, not adjacent to haulage roads	1.3
Moderately Serious	Any slope of a permanent or semi-permanent nature	1.6
Very Serious	Critical permanent slopes carrying major haulage roads or underlying permanent mine installations	2.0

During an analysis in FLAC3D using SlopeX, a number of plots are automatically generated. This includes a plot that shows a ‘group’ defined based on the velocity as above. Typically, during the analysis of slope stability, one would rely on plots of either the yielding or the development of shear strain. However, as shown in Fig. 8a and Fig. 8b the interpretation of a shear surface requires experience in some materials. Instead as discussed above, the definition of failure using velocity, provides a clear image of failure (Fig. 8c), which is labelled with group name (Fig. 8e).

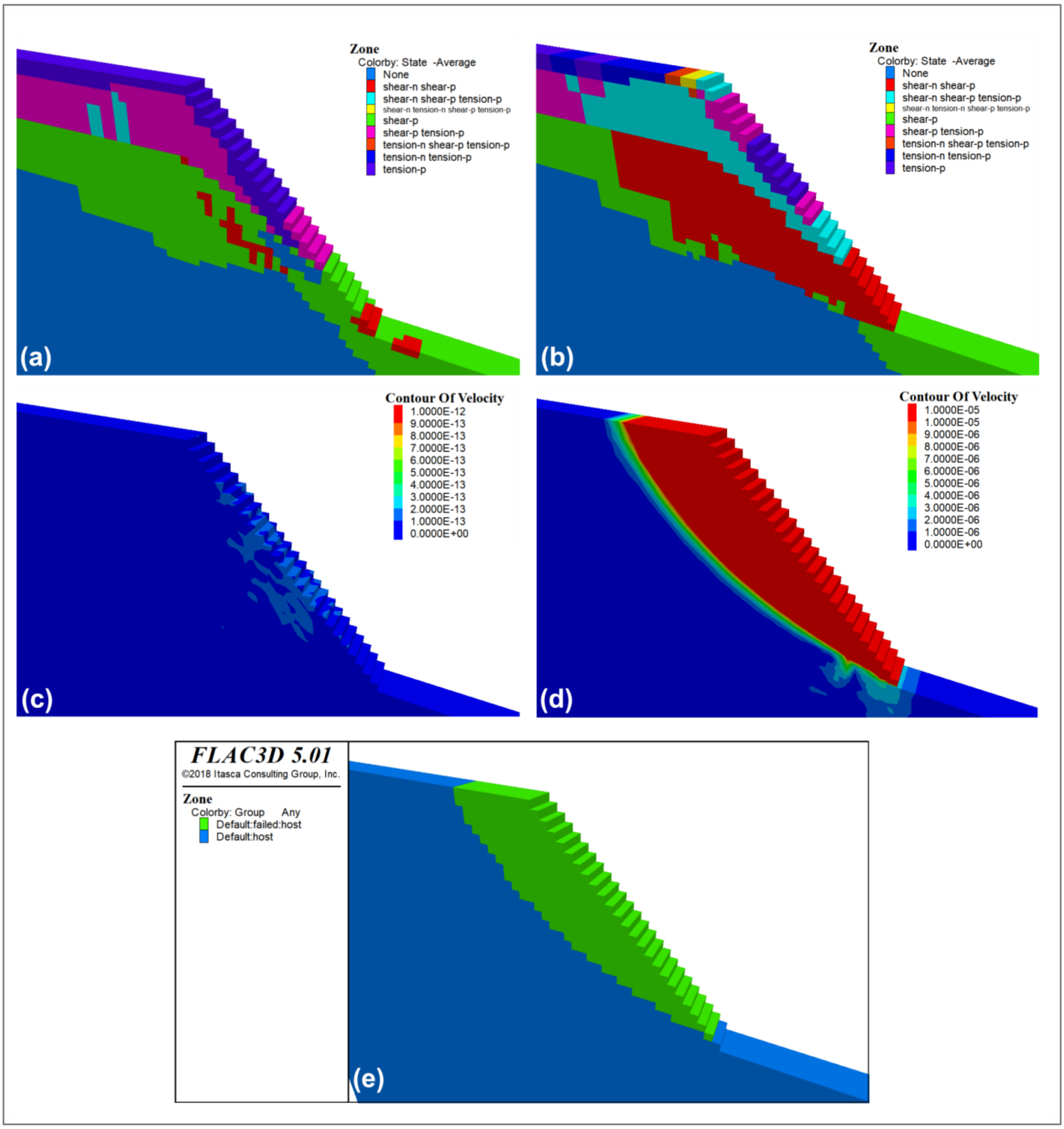

Fig. 8 Example of failure criteria defined within SlopeX, demonstrated by a 200 m high slope in Rock Mass B with a slope angle of 45°, (a) shows the failure state when SRF = 1.67; (b) the failure state when SRF = 1.67; (c) negligible velocity when SRF = 1.67; (d) velocity when SRF = 1.67; (e) subsequent failure flag added to represent slope failure at an SRF of 1.67

2.4 Comparison with CaveHoek

As discussed in Section 1.3, the IUCM has been verified against over 100 mining cases worldwide. To provide an example of a similar analysis in two dimensions, the analysis presented by Cancino et al. (2018) has been repeated. As previously shown in Fig. 5, Cancino et al. (2018) analysed a rock mass of ‘moderate quality’, suggesting the FS for a 500 m high slope with a slope angle of 45°, to be between 2.1 and 2.2 for deep-seated failure.

An analysis with the same input parameters (Table 3), is developed and interpreted using SlopeX, suggests a FS of 2.08 (Fig. 9a). This approach closely matches that presented by Cancino et al. (2018), and the result from SlopeX was resolved without the sensitivity analyses that was necessary in the case of the modelling by Cancino et al. (2018). This supports analysis using IUCM, allowing a rapid analysis of overall and inter-ramp stability necessary for the development of slope stability curves.

Table 3 Model inputs for a ‘moderate’ rock mass used by Cancino et al. 2018

Parameter		Value
Density	ρ (t/m^3)	2.7
Intact Young’s Modulus	E_i (GPa)	25
Geological Strength Index	GSI	45
Hoek Brown Constant	m_i	15
Intact uniaxial compressive strength	UCS (MPa)	60

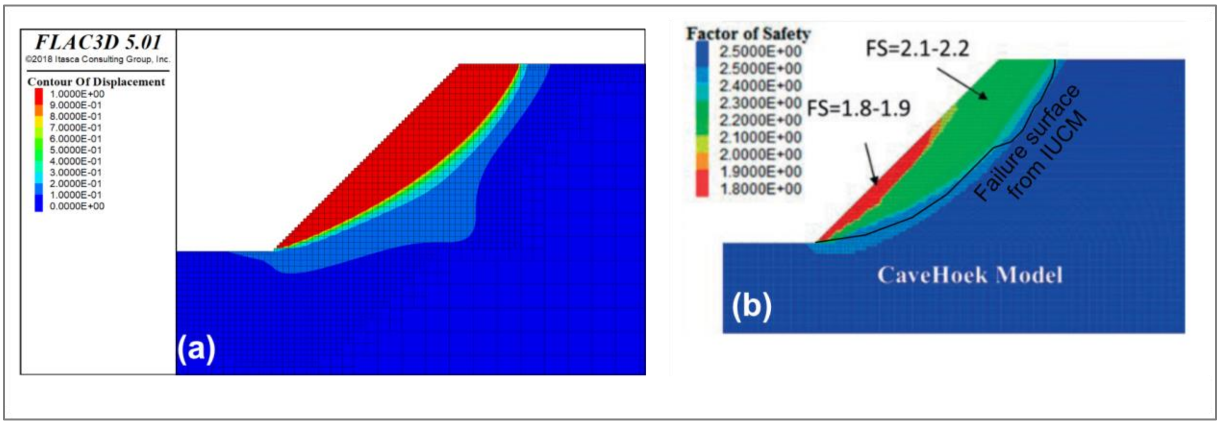

Fig. 9 500 m high slope with a 45° slope angle, (a) analysis in with IUCM in which an SRF of 2.08 is applied; (b) analysis from Cancino et al (2018) using CaveHoek, with

3 Analysis Results

3.1 Rock Mass A

Analyses were completed with slopes ranging from 200 m to 1000 m in height and with slope angles between 45° and 60°. An example of one result is shown in in Fig. 10, which demonstrates the ability of the model to capture the progressive development of a failure mechanism.

Using the results from the analyses, a number of charts are developed which allow the derivation of a design curve for a desired FS. Subsequently, these design curves can be plotted onto the slope angle versus slope height chart, as presented in Fig. 10 for Rock Mass A. Note that the design curve for a FS of 2.0 has been derived from a sufficient number of data points. Further analyses are recommended to fully define the curves that are currently indicated for a FS of 1.6 and 1.3. Note that although a curve is tentatively indicated for a FS of 1, the FS 1 line is not a design curve because any geometry in which the FS is <1.3 is considered to be unacceptable.

An example of where further analysis is required is shown in the case of a slope that is 800 m high with a 50° angle (circled in purple in Fig. 10); the FS is 1.6 however it is not within the appropriate area on the chart. Despite the further analysis that is required, the data presented provided an indication as to the minimum number of analyses to define the slope stability curves.

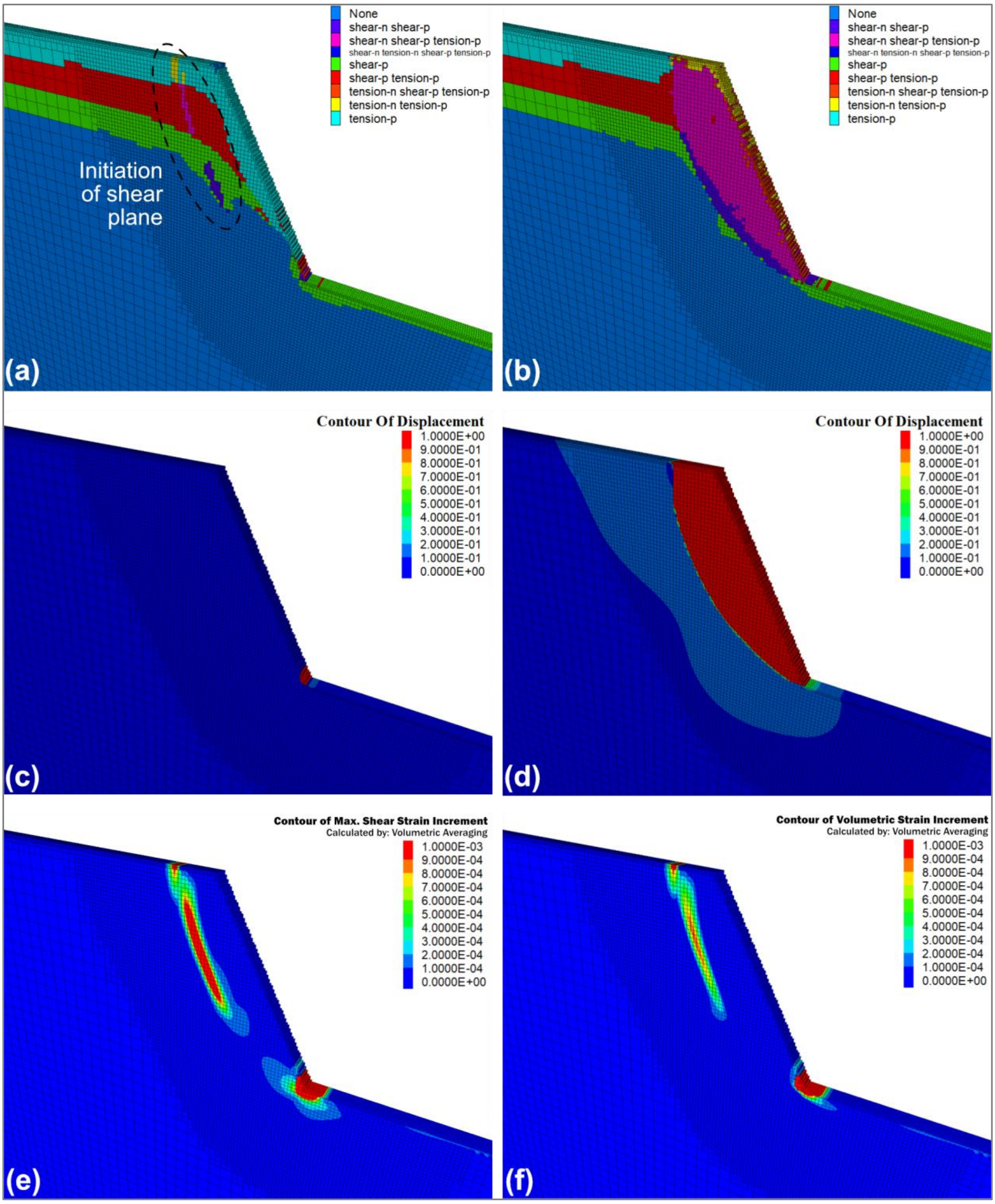

Fig. 10 800 m high slope with a slope angle of 60° in Rock Mass A, (a) showing yielding with initiation of shear plane at a SRF of 1.04; (b) yielding at SRF of 1.05; (c) a clear definition of failure with minimal displacement at a SRF of 1.04; (d) widespread displacement at SRF of 1.05; (e) development of shear strain at a SRF of 1.04; (f) volumetric strain at a SRF of 1.04

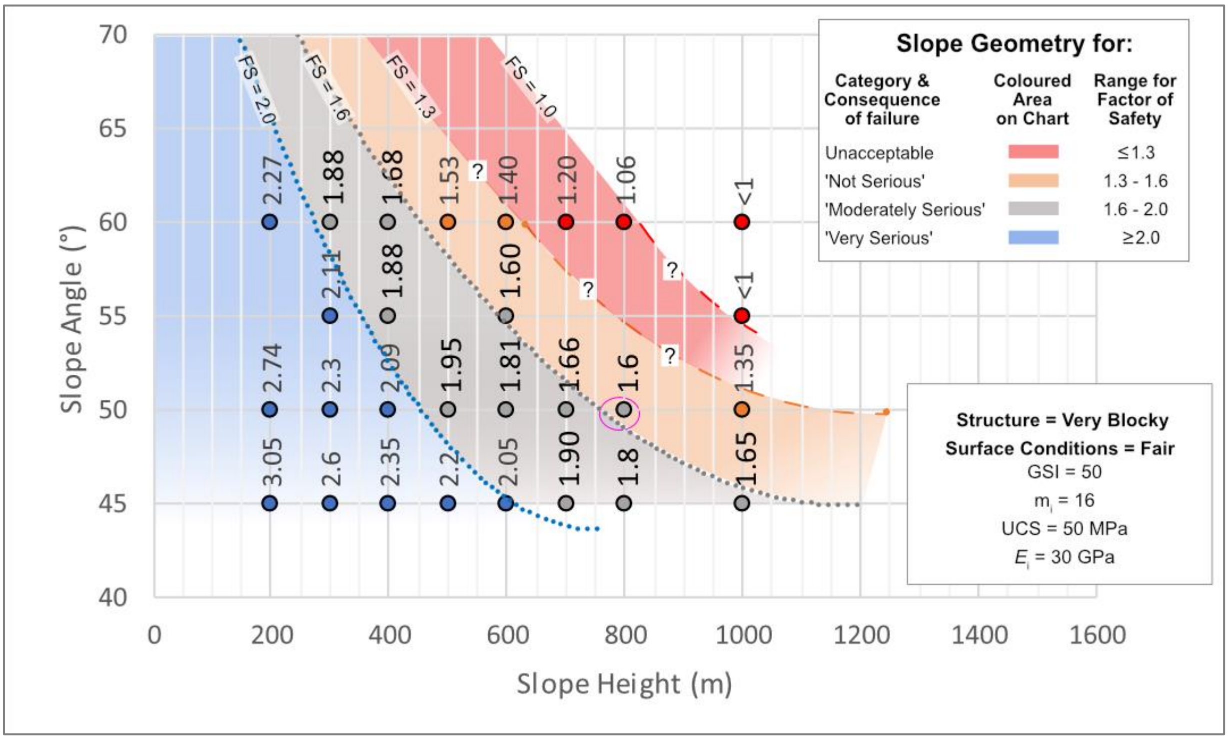

Fig. 11 Slope Stability Curves for Rock Mass A; design curves for FS of 2.0 and 1.6 are confirmed, lower FS are approximated; the FS values are labelled on each point

As discussed in Section 1.3, anisotropy can be incorporated using SlopeX. To understand the potential reduction in FS, a preliminary analysis was completed with a moderate anisotropic factor of 4.5. This value represents the magnitude by which the strength reduces, in the orientation of the anisotropy. The anisotropy was orientated to dip out of the face at an angle of 45° with the rock mass having a m_i of 8 in the direction of anisotropy. In these conditions the FS is decreased significantly (from 2.29 to 1.28), and the depth of displacement decreases (Fig. 12). A more detailed study of anisotropy and the subsequent influence on the slope stability curves, is a focus for further study.

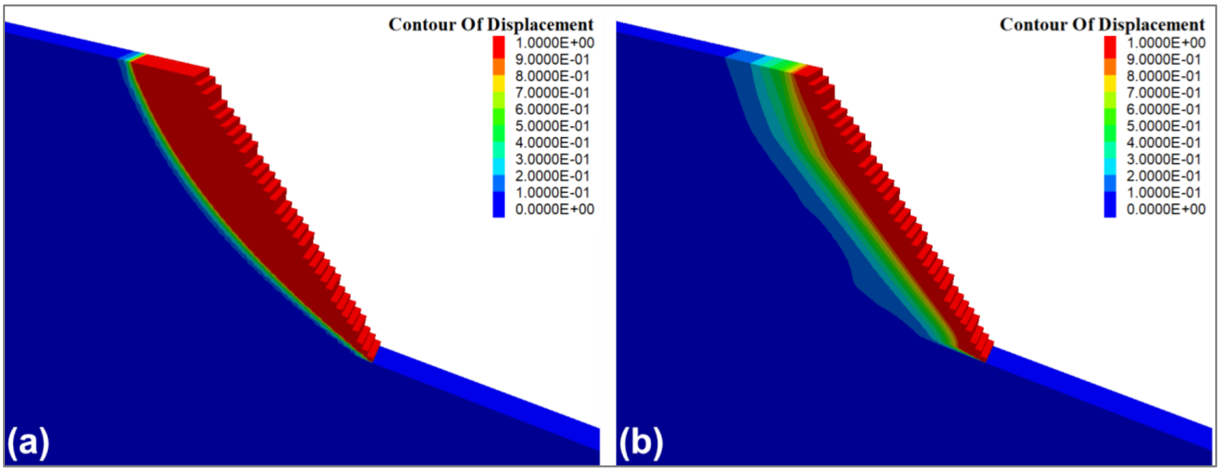

Fig. 12 300 m high slope with a slope angle of 50° in Rock Mass A, (a) showing displacement at the FS of 2.29 in an isotropic model; (b) anisotropic model with subsequent decrease in FS to 1.28 and decrease in the depth of displacement

3.2 Rock Masses B and C

A more streamlined approach was taken for Rock Mass B and Rock Mass C, using the minimum number of analyses required. Analyses were completed with slopes ranging from 100 m to 700 m in height and with slope angles between 40° and 60° for Rock Mass B.

In the same way as for Rock Mass A, further analyses are recommended to fully define the curves that are currently indicated. However, Fig. 13 shows the most complete image for the three rock masses, with only slight modifications necessary for the design curve that defines the FS of 1.3 (the FS for a 200 m high with a 50° slope angle is circled in purple as an example of where further analysis is required).

Fig. 14 presents the data for Slope Stability Curve for Rock Mass C which was completed as an academic exercise. The slope heights that are indicated in Fig. 14 are excessive, and it is suggested that it is unfeasible for a rock mass may be constituted entirely of one single strong unit without any faults, weak lithologies or anisotropy.

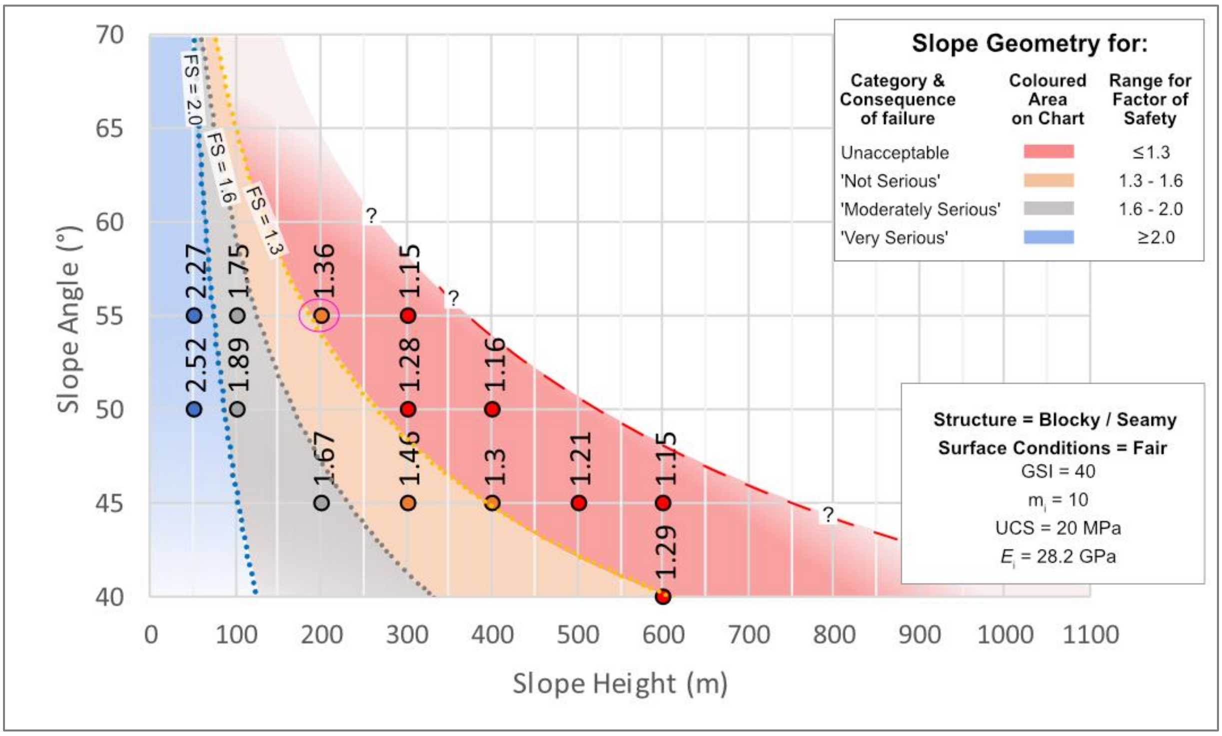

Fig. 13 Slope Stability Curves for Rock Mass B; design curves for a FS of 2.0 and 1.6 are confirmed, while lower FS are approximated; the FS values are labelled on each point

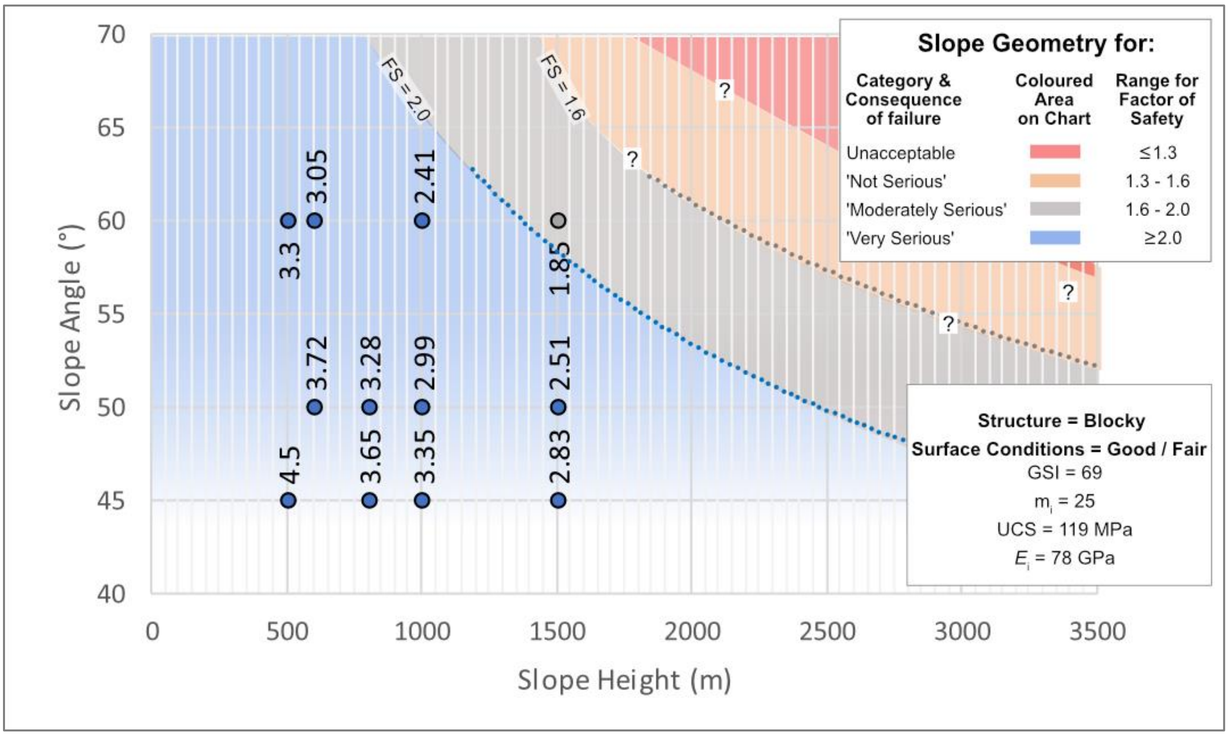

Fig. 14 Slope Stability Curves for Rock Mass C; design curves for a FS of 2.0 is confirmed, while lower FS are approximated; the FS values are labelled on each point

3.3 Analysis in 3D using SlopeX

As discussed in above and previously in Section 1.2, the Slope Stability Curves that have been presented were developed using modelling in two-dimensions. A pit design was analysed using the properties from Rock Mass B, to provide an example of the three-dimensional capability of SlopeX.

The geometry that was chosen is a 386 m high slope, with overall angles of between 33° and 37°. The steepest inter-ramp angles vary with 57° for a 72 m. As presented in Fig. 15, the FS for the overall slope angled at 42°, is at a value of 1.6 where the failure plane is projected to occur over a height of 314 m. This agrees with the slope stability curve for Rock Mass B (Fig. 13).

In the steeper inter-ramp case, the FS is projected to be 1.4. The slope stability curve suggests a value in the 'Moderately Serious' range, which is not in agreement. In this case it would be suggested that a more detailed numerical model should be developed in this area, to fully understand the mechanism. This emphasises the intention that the stability curves should only be used as an initial guide for assessing stability.

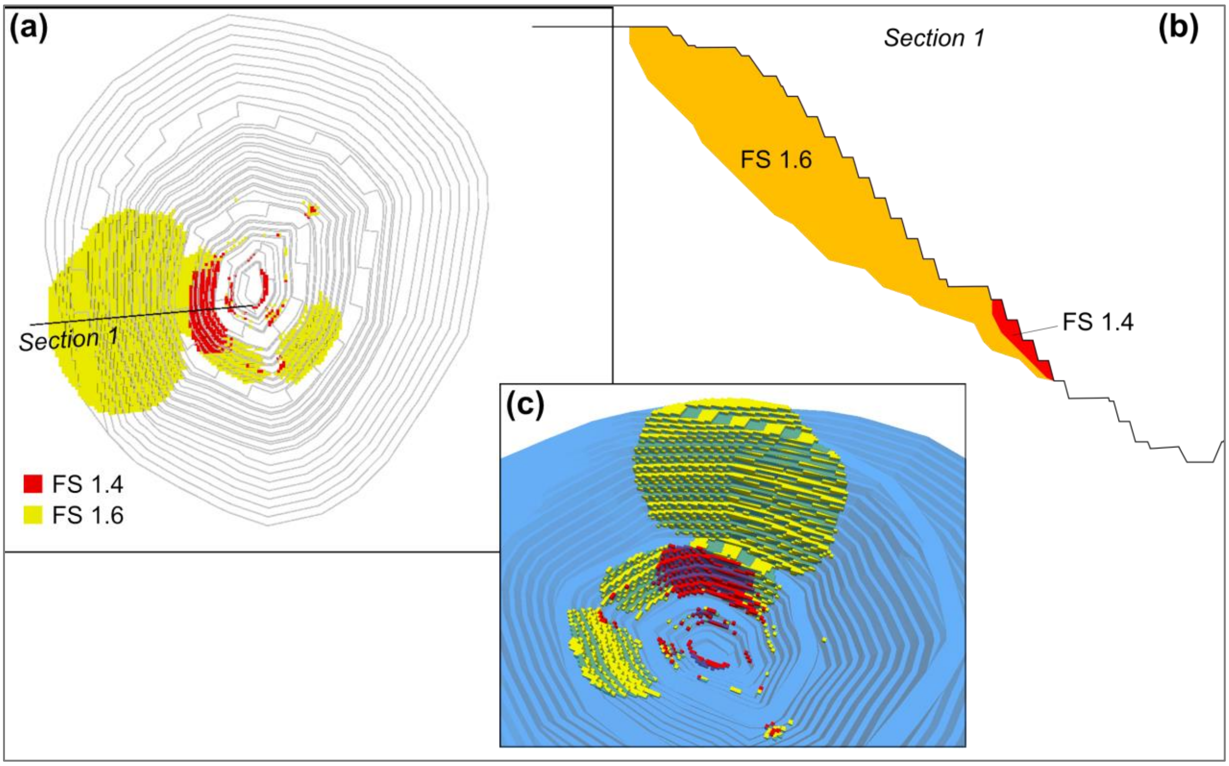

Fig. 15 Analysis of a 386 m deep pit with Rock Mass B properties, showing an inter-ramp slope with a FS of 1.4 and an overall slope with a FS of 1.6; (a) presented in plan view; (b) presented in sectional view; (c) presented in perspective view

4 Discussion

The concept of 'Slope Stability Curves' has been introduced as empirical design charts that represent specific rock mass conditions. They are intended to be an initial guide for assessing overall stability, or as a reference to study the influence of inputs on analysis results. As discussed by Read and Stacey (2009), design charts can be useful during desktop and pre-feasibility studies. However, based on their experience the authors would suggest limiting the sole application of design charts to desktop studies. Instead it is recommended that conventional analytical and numerical tools are used to explicitly represent the slope conditions, perhaps with initial guidance from empirical approaches, such as a slope stability curve.

The slope stability curves have been developed using SlopeExamine (also known as SlopeX), which provides the opportunity to rapidly develop a model of slope in FLAC3D. The inbuilt strength criterion (IUCM) available via SlopeX, allows confinement-controlled softening/hardening of cohesion and friction, confinement-controlled changes in the dilation angle, and porosity-controlled modulus softening. A comparison has been made to a similar analysis that was completed using another approach (CaveHoek), demonstrating a similar result.

Three rock masses have been chosen that can be defined on the Hoek-Brown classification chart. A set of slope stability curves have been developed for each of the rock masses, as a demonstration of the approach. In addition, a preliminary analysis was completed in Rock Mass A, which included an unfavourable anisotropy. The result indicates a significant reduction in the FS, which exemplifies the importance of anisotropy. It can be suggested that at present, practitioners rely on the blast damage to weaken the rock mass, as opposed to explicitly considering the strength implications of either anisotropy or a fracture network.

The analyses that are presented form the basis for future study, in which groundwater and anisotropy will be introduced. This will allow slope stability curves to be developed for a wide range of conditions, not only in fractured rock, but perhaps also for soft rock soil and engineered slopes. In the case of fractured rock, it is suggested that attempts should be made to develop a relationship between the Hoek-Brown and GSI inputs and the resulting stability curves, to allow the development of a new empirical system.

References

Alejano LR, Alonso E. (2005) Considerations of the dilatancy angle in rocks and rock masses. Int J Rock Mech Min Sci, 42(4):481–507. 10.1016/j.ijrmms.2005.01.003

Cancino C, Álvarez C, Orrego C, Díaz M, Ledezma R (2018) Applicability of Strain Softening Models to Slope Stability Analyses. Slope Stability 2018, Seville, Spain. 10-13 April 2018

Carter TG (2018). Suggested Standards for Improving Structural Geological Definition for Open Pit Slope Design. Slope Stability 2018, Seville, Spain. 10-13 April 2018

Ford A, Lucas D, Vakili A (2020) Validation of the Improved Unified Constitutive Model (IUCM) for Open Pit Applications. Slope Stability 2020, Perth, Australia, 12-14 May 2020

Haines A, Terbrugge PJ (1991). Preliminary estimate of rock slope stability using rock mass classification systems. 7th Congress of International Society of Rock Mechanics, Aachen, Germany, 16-20 September 1991

Hoek E, Bray JW (1981) Rock Slope Engineering, 3rd ed. The Institute of Mining and Metallurgy, London.

Lucas DS, Vakili, A, Hutchinson BJ (2020) Slope design and control of rock fall hazards in a challenging structural setting at the Kanmantoo copper mine, South Australia. Slope Stability 2020, Perth, Australia, 12-14 May 2020

Lorig L, Varona P (2000) Practical Slope Stability Analysis Using Finite Different Codes, in Slope Stability in Surface Mining. Society for Mining, Metallurgy and Exploration Inc.(SME), Littleton, USA

McKenzie CK (2016) Blasting near open pit wall. The First Asia Pacific Slope Stability in Mining (APSSIM) Conference, Brisbane, Australia, 6-8 September 2016

Pine RJ (1992) Risk Analysis design applications in mining geomechanics. Trans. Instn. Min. Metall. Section A (Min. Industry). 101: A149–A 158

Read J, Stacey P (2009) Guidelines for Open Pit Design, CSIRO Publishing, Collingwood, Vic.

Sjöberg J (1999) Analysis of Large Scale Rock Slopes. PhD thesis at Lulea University of Technology

Silva GR, Gómez PP (2015) Towards a Mechanically Based Definition of the Disturbance Factor Using The “Slope Model” Lattice Code. 8th South American Congress on Rock Mechanics, Buenos Aires, Argentina, 15–18 November 2015

Vakili A (2016) An improved unified constitutive model for rock material and guidelines for its application in numerical modelling. Computers and Geotechnics 80: 261-282. 10.1016/j.compgeo.2016.08.020

Vakili A, Watson J, Abedian B, Styles T (2020) SlopeX – a Plug-in to Simplify and Fast-Track Advanced Numerical Modelling for Open Pit Applications. Slope Stability 2020, Perth, Australia, 12-14 May 2020